International Journal of Research
Available at https://edupediapublications.org/journals
p-ISSN: 2348-6848
e-ISSN: 2348-795X
Volume 03 Issue 18
December 2016

Study of Synchronization Methods for Grid Faults

[1] K.AKHILA,[2] P. SARALA

[1]M.Tech., EPS, Dept. of EEE, Dr. K. V. S. W, Emal.id akhila.kvsw@gmail.com, KURNOOL

[2]Associate Professor, M.Tech(ph. D); EPS, Dept. of EEE, Dr. K. V. S. W, KURNOOL

Abstract—The genuine system code necessities for the lattice association of conveyed era systems, for the most part wind and photovoltaic (PV) systems, are turning out to be exceptionally requesting. The transmission system operators (TSOs) are particularly worried about the low-voltage-ride-through necessities. Arrangements in view of the establishment of STATCOMs and element voltage controllers (DVRs), and in addition on cutting edge control functionalities for the current power converters of disseminated era plants, have added to improve their reaction under broken and bended situations and, subsequently, to satisfy these prerequisites. So as to accomplish tasteful outcomes with such systems, it is important to rely on exact and quick lattice voltage synchronization calculations, which can work under lopsided and twisted conditions. This paper examines the synchronization ability of three propelled synchronization systems: the decoupled twofold synchronous reference outline stage bolted circle (PLL), the double second request summed up integrator PLL, and the three-stage improved PLL, intended to work under such conditions. Albeit different systems in light of recurrence bolted circles have likewise been created, PLLs have been picked because of their connection with dq0 controllers. In the accompanying, the diverse calculations will be introduced and discretized, and their execution will be tried in an exploratory setup controlled with a specific end goal to assess their accuracyand usage highlights.

Index Terms—Electric variable measurements, electrical engineering, frequency estimation, frequency-locked loops,harmonicanalysis, monitoring, synchronization.

INTRODUCTION

The power share of renewable vitality based era systems should achieve 20% by 2030, where wind and photovoltaic (PV) systems are thought to be the most cases of incorporation of such systems in the electrical system. The expanded infiltration of these innovations in the electrical system has strengthened the officially existing worry among the transmission system administrators (TSOs) about their

impact in the network dependability; as an outcome, the lattice association norms are turning out to be increasingly prohibitive for conveyance era systems in all nations. In the grid code requirements (GCRs), unique limitations for the operation of such plants under network voltage blame conditions have picked up an extraordinary significance. These prerequisites decide the blame limits among those through which a lattice associated era system should stay associated with the system, offering ascend to particular voltage profiles that indicate the profundity and freedom time of the voltage lists that they should withstand. Such prerequisites are known as low voltage ride through (LVRT) and are portrayed by a voltage versus time trademark.

In spite of the fact that the LVRT prerequisites in the distinctive gauges are altogether different, the main issue that era systems must bear the cost of when voltage hang happens is the impediment of their transient reaction with a specific end goal to keep away from its defensive detachment from the system. This is the situation, for example, of settled speed wind turbines in view of squirrel confine acceptance generators, where the voltage drop in the stator windings can lead the generator to an over speed stumbling. In like manner, variable speed wind control systems may lose controllability in the infusion of dynamic/responsive power because of the separation of the rotor side converter under such conditions. Moreover, PV systems would likewise be influenced by a similar absence of current controllability.

Arrangements in light of the improvement of helper systems, for example, STATCOMs and dynamic voltage regulators (DVRs), have assumed an unequivocal part in upgrading the fault ride through (FRT) capacity of conveyed era systems, as showed in. Moreover, propelled control functionalities for the power converters have likewise been proposed. Regardless, a quick identification of the blame adds to enhancing the impacts of these arrangements; in this manner, the synchronization calculations are urgent.

In specific nations, the TSOs likewise give the dynamic/receptive power example to be infused into the system amid voltage list; this is the situation for the German E-on and the Spanish Red Electrica Espanola ((REE). This pattern has been trailed by whatever remains of the TSOs; in addition, it is trusted that this operation necessity will be developed, and particular requests for adjusted and lopsided droops will emerge in the accompanying renditions of the network codes around the world.

With respect to operation of the disseminated era systems under adjusted and lopsided blame conditions, important commitments, can be found in the writing. These arrangements depend on cutting edge control systems that need precise data of the network voltage factors keeping in mind the end goal to work appropriately, something that has provoked the significance of lattice synchronization calculations. In power systems, the synchronous reference outline PLL (SRF PLL) is the most amplified strategy for synchronizing with three-stage systems. By the by, in spite of the way that the execution of SRF PLL is palatable under adjusted conditions, its reaction can be deficient under unequal, broken, or twisted conditions.

In this venture, three enhanced and propelled system synchronization systems are considered and assessed: the decoupled twofold synchronous reference outline PLL (DDSRF PLL) , the dual second order generalized integrator PLL (DSOGI PLL), and the three-stage improved PLL (3phEPLL) . Their execution, computational cost, and unwavering quality of the abundancy and stage identification of the positive grouping of the voltage, under uneven and mutilated circumstances, have been assessed by lattice blame examples separated from and , which have been recreated in a genuine scaled electrical system.

In the accompanying areas, the discrete representation of each PLL will be definite, because of its extraordinary significance in the last usage of the control, after a brief portrayal of the distinctive structure. At long last, their conduct will be tried in a trial setup, and their execution will be talked about, especially considering the exactness of the positive-grouping location and their computational cost while considering distinctive defective situations, covering the reaction before hangs, recurrence changes, and symphonious resistance.

GRID CODE REQUIREMENTS:

To research the dynamic conduct of DG systems, the general network code necessities are returned to in this area. Network codes have been upheld for nations like USA, Germany, Spain, Denmark, China and Canada which have significant era. The significant necessities of ordinary matrix codes for operation and lattice association of DG systems are abridged as takes after Voltage control: This implies by the association of DG, the voltage at the PCC should not go outside a predetermined range. system Frequency: Likewise, the recurrence deviations might likewise not go outside a predetermined range. Synchronization: While synchronizing a DG with a zone electric power system (EPS) it might not bring about a voltage change of more than ± 5% of the overarching voltage level at the PCC. Observing arrangements: A DG arrangement of rating 250 kW or bigger might have arrangements for the checking of association status and genuine and responsive power yield at the purpose of DG association. Detachment gadget: Whenever required by territory EPS working practice, a confinement gadget might be situated between the DG unit and the region EPS. Establishing: There ought to be a legitimate coordination among the establishing plan and the establishing deficiency security of DGs with the EPS administrators. Voltage unsettling influences: During any anomalous voltage condition, a DG should stop to invigorate the EPS inside a predetermined clearing time. Recurrence aggravations: Likewise, if the recurrence is outside the typical range a DG should stop to empower the EPS inside a predetermined time. Loss of synchronization: A DG of 250 kW or bigger might be outfitted with loss of synchronism security capacities to detach the DG from the territory EPS immediately. Reconnection: After a beyond the field of play aggravation, a DG should stop to stimulate the region EPS, and might stay disengaged until the territory EPS voltage and recurrence have come back to and kept up ordinary extents for 5 minutes. 2.2.11 Anti-Islanding A DG should identify the island condition and stop to invigorate the region EPS inside 2

seconds of the development of an island. Sounds: The passable voltage symphonious contortion is determined at the PCC. It is regularly required that the most extreme voltage add up to symphonious bending is 5% and greatest individual recurrence voltage consonant is 3% of the crucial segment. DC current infusion: A DG and its interconnection system might not infuse dc current more prominent than 0.5% of its evaluated yield current into the range EPS at the PCC. Flash: A DG should not make questionable glimmer for clients on the territory EPS.

GRID SYNCHRONIZATION ALGORITHMS:

Few of the different network synchronization calculations that are proposed in writing are:-

Zero Crossing Detectors:

A zero intersection indicator (ZCD) is a circuit that recognizes a move of air conditioning voltage starting with one extremity then onto the next. At whatever point a move from positive to negative happens a heartbeat is created demonstrating 0 degree and in like manner 180 degree for the turn around case. The execution of ZCD is seriously influenced by power quality wonders.

Phased Locked Loop:

A Phased Locked Loop (PLL) is a system which synchronizes its yield motion with a given information flag or reference flag both in recurrence and in stage. It is a non-straight shut circle control which naturally changes the recurrence of a controlled oscillator relying upon the recurrence and period of the info flag to such an extent that the yield is coordinated both in recurrence and stage with the reference or the information flag.

The fundamental segments of a PLL are

A phase finder which thinks about the info/reference flag and the yield flag and produces a mistake flag.

A circle channel which expels undesirable sounds terms from the blunder flag.

A voltage controlled oscillator (VCO) which creates the yield flag whose recurrence changes around a focal recurrence relying upon the yield of the circle channel. The piece graph of a PLL is appeared underneath in Figure.1.1.

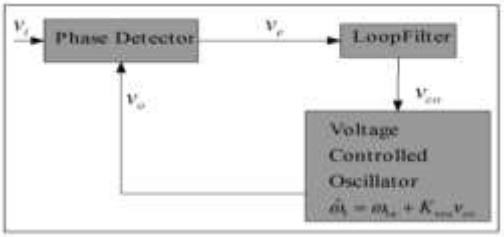

Fig.1.1.Block diagram of PLL

The various kinds of PLL techniques are:-

1.2.3. Linear PLL: Linear PLL (LPLL) is mainly used for single phase voltage. It has a mixer which is used as a phase differentiator which gives a signal proportional to the difference between the phases of the input and the output signal. This error signal also contains components at frequencies which are even multiples of the input frequency. The loop filter removes the harmonic components and only the proportional component is passed on to the voltage controlled oscillator according to which the VCO output is generated.

The whole model is shown by a block diagram in Figure.1.2.

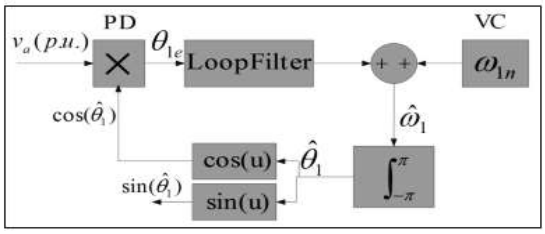

Fig.1.2. Block diagram of linear PLL

The phase differentiator output is:-

=

Now assuming that the PLL is locked in st

,

Where V is the input signal, is the input frequency, and the terms with (^) represent the output signal. This equation shows that the result has information about the phase error along with some other harmonic components which are removed by the Loop Filter.

1.2.4. Synchronous Reference Frame PLL: A synchronous Reference Frame PLL (SRF PLL) is mainly used for tracking the phase angle in case of 3-phase signals which works in a similar way as a linear PLL with only difference in the Phase Detector (PD) block. It uses Park's Transformation of a 3-phase signal as the PD.

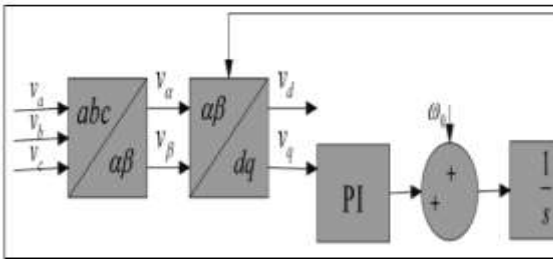

Figure.1.3.Block diagram of synchronous reference frame PLL

Fig. 1.3. shows the block diagram of a SRF PLL in which va, vb, vc are the components of a 3-phase signal. First block in the figure is Clarke's Transformation which translates a 3- phase voltage vector from the abc natural reference frame to the αβ stationary reference frame. The second block is the Park's Transformation which translates the αβ stationary reference frame to rotating frame. A Proportional Integrator (PI) controller is used as loop filter.

1.2.5. Decoupled Double Synchronous Reference Frame (DSRF) PLL:

The DSRF PLL is a blend of two routine SRF PLLs. These two casings are isolated by a union circuit which is appeared in figure 1.4. The voltage vector is deteriorated into positive and negative grouping vectors and these parts are meant by and separately as appeared in figure1.5. The piece chart of DSRF PLL, demonstrates that the α and β pivot segments both contain the data of the positive succession and negative arrangement which makes it hard to recognize the positive grouping part. The two PLLs work freely, turning with positive bearing and negative course individually and distinguish the positive arrangement and negative succession at the same time.

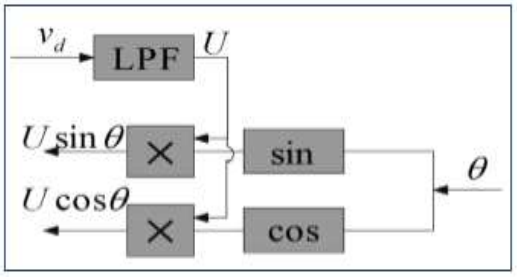

Figure.1.4.

Synthesis circuit used in DSRFPLL

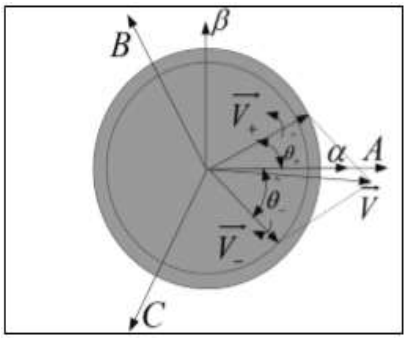

Figure.1.5. Voltage vector decomposition (unbalanced voltage)

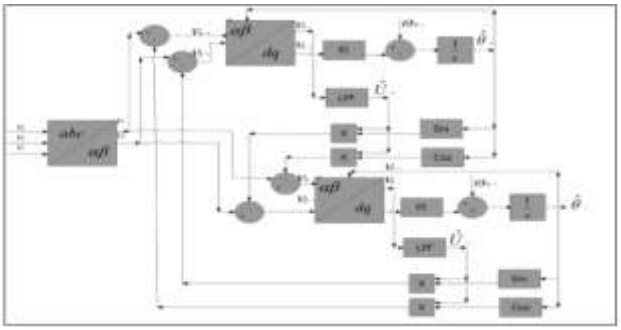

Figure.1.6.

Block diagram of DSRFPLL

At the point when the three stage matrix voltage is unequal, the principal positive-grouping voltage vector shows up as a DC voltage on the dq+1 tomahawks of the positive arrangement SRF and as air conditioning voltages at double the essential utility recurrence on the dq-1 tomahawks of the negative succession SRF. Unexpectedly, the negative grouping voltage vector will bring about a dc segment on the negative succession SRF and an air conditioner swaying on the positive arrangement SRF. Since the adequacy of the swaying on the positive grouping SRF matches to the DC level on the negative succession SRF and the other way around, a decoupling system is connected to signals on the dq positive/negative SRF tomahawks with a specific end goal to offset such air conditioning motions. Low pass channels are responsible for removing DC part from the flag on the decoupled SRF tomahawks. These DC segments gather the data about the adequacy and stage edge of the positive and negative succession segments of the matrix voltage vector.

The circle controller of the DDSRF-PLL takes a shot at the decoupled q-pivot flag of the positive arrangement SRF (Uq+1). The flag is free of air conditioning parts because of the impact of the decoupling cells and the band width of the circle controller can be therefore expanded.

ENHANCED PLL:

Enhanced phase-locked loop (EPLL) is a recurrence versatile nonlinear synchronization approach. The square graph of EPLL is appeared in figure. Its significant change over the customary PLL lies in the PD component which permits more adaptability and gives more data, for example, adequacy and stage edge. There are three autonomous interior parameters K , Kp Kv and Ki Kv . Parameter K overwhelmingly controls the speed of the abundancy merging. Kp Kv and Ki KV control the rates of stage and recurrence merging.

EPLL can give higher level of resistance and lack of care to clamor, sounds and unbalance of the information flag. It is a viable strategy for synchronization of the matrix interfaced converters in dirtied and

variable-recurrence situations. What's more, EPLL can give the 90 degrees move of the info flag. Thusly, it is an alluring arrangement in some single stage system applications.

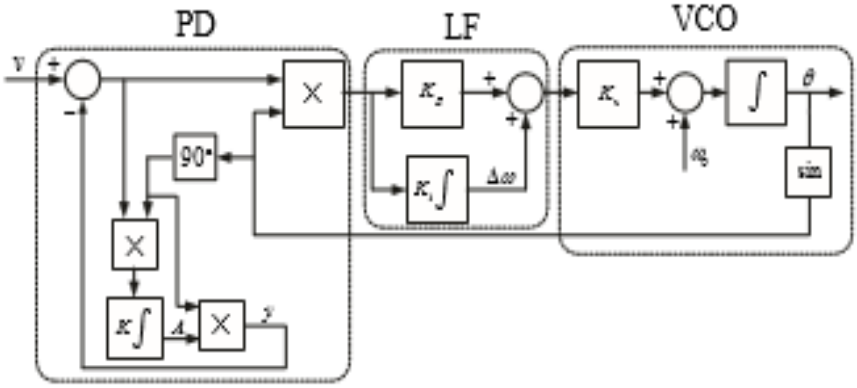

Figure.1.9. Block diagram of single phase EPLL

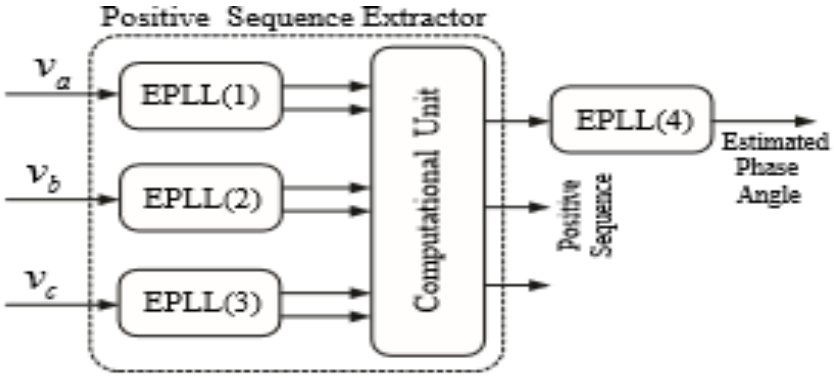

Figure.1.10. Block diagram of 3-PH EPLL

GRID SYNCHRONIZATION SPECIFICATIONS BASED ON GCR:

Despite the fact that few works are distributed inside the field of matrix synchronization, every one of them are fixated on breaking down the individual element execution of every proposition, without first deciding a period reaction window inside the dynamic conduct of the system under test, which would be thought to be tasteful.

To assess the reaction of the lattice synchronization topologies under test, a typical execution prerequisite for every one of the structures has been set up in this segment, considering the necessities that can be gotten from the LVRT necessities.

Regardless of the way that the identification of the blame can be completed with less difficult calculations, the significance of cutting edge lattice synchronization systems lies in the need of having precise data about the extent and period of the network voltage amid

International Journal of Research
Available at https://edupediapublications.org/journals
p-ISSN: 2348-6848
e-ISSN: 2348-795X
Volume 03 Issue 18
December 2016

the blame, keeping in mind the end goal to infuse the receptive power required by the TSO.

In the German standard, it is expressed that voltage control must occur inside 20 ms after the blame acknowledgment, by giving a responsive current on the low voltage side of the generator transformer to no less than 2% of the evaluated current for every percent of the voltage plunge, as appeared in Figure. 100% receptive power conveyance must be conceivable, if fundamental.

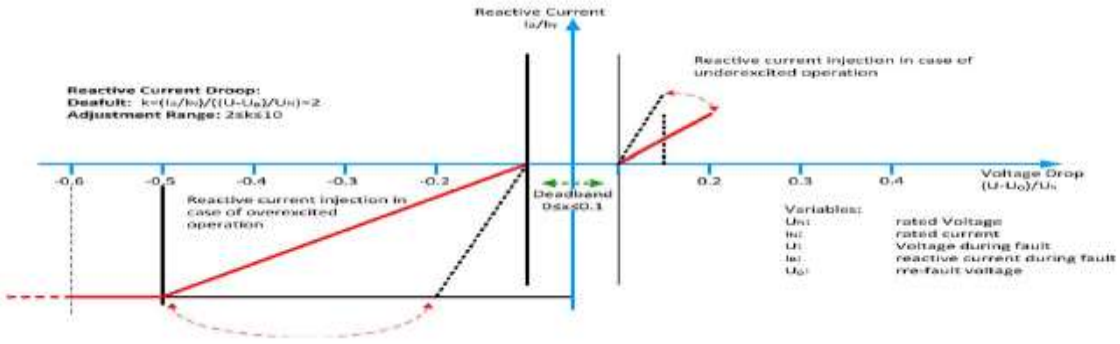

2.1.E-on voltage support requirement in the event of grid fault

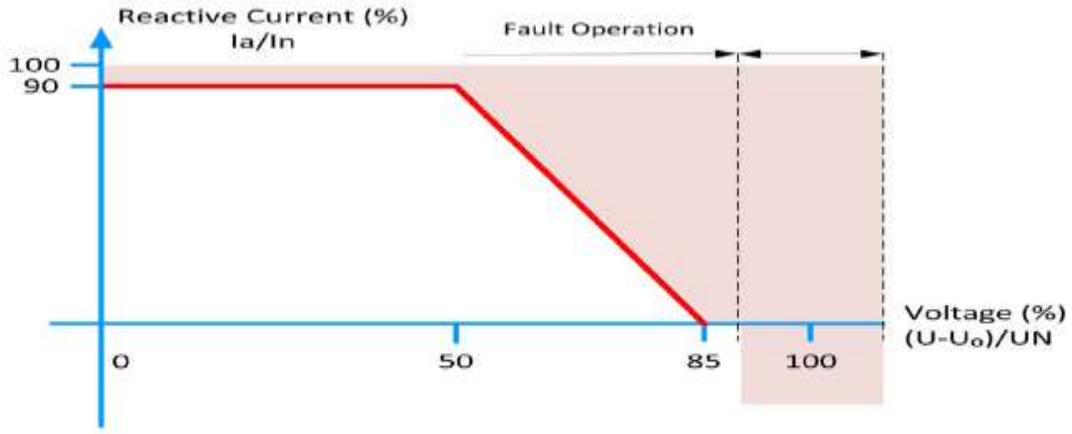

Figure.2.2.REE voltage support requirement in the event of grid fault.

A comparable condition is given in the Spanish network code, where the wind control plants are required to quit drawing inductive responsive power inside 100 ms of a voltage drop and have the capacity to infuse full receptive power after 150 ms, as appeared in Fig. 2.2.

Considering these requests, this paper will consider that the estimation of the voltage conditions will be completed inside 20–25 ms, as this objective licenses it to satisfy the most prohibitive necessities, as far as dynamical reaction, accessible in the

lattice codes. This condition will be stretched out to recurrence estimation; in spite of the fact that this parameter is more identified with optional control calculations than LVRT, a similar time window somewhere around 20 and 25 ms will be considered in this work for the recognition of the aggravation.

.2.2. DESCRIPTION OF DECOUPLED DOUBLE SYNCHRONOUS REFERENCE FRAME PLL:

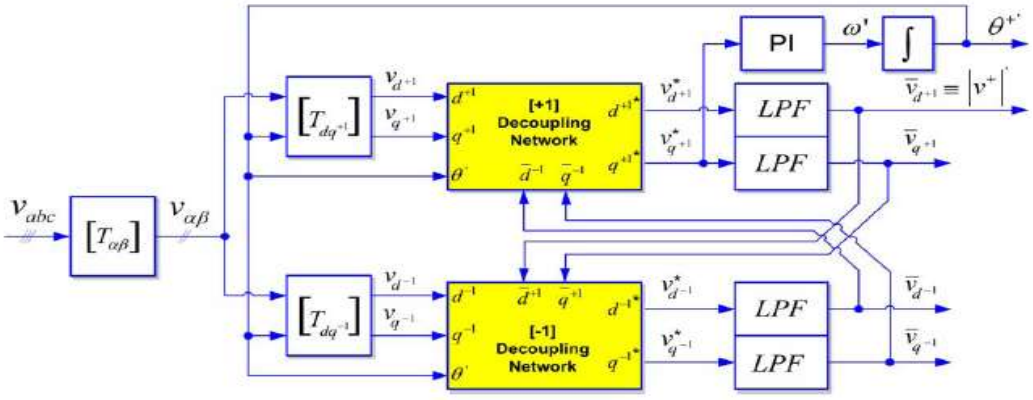

Fig. 2.3. DDSRF-PLL block diagram.

A considerable lot of the positive-grouping recognition calculations depend on SRF PLLs. In spite of having a decent reaction under adjusted conditions, their execution gets to be distinctly inadequate in unequal defective matrices (95% of cases), and their great operation is exceptionally adapted to the recurrence strength, which is contradictory with the possibility of a strong synchronization system.

Many creators have talked about various propelled models, which can beat the issues of the traditional PLL, utilizing recurrence and abundancy versatile structures which can manage unequal, flawed, and symphonious contaminated matrices.

The DDSRF PLL was created for enhancing the ordinary SRF PLL. This synchronization system misuses two synchronous reference outlines turning at the central utility recurrence, one counterclockwise and another clockwise, with a specific end goal to accomplish an exact identification of the positive-and negative-succession segments of the network voltage vector when it is influenced by unequal matrix issues. The chart of the DDSRF PLL is appeared in Fig.2.3.

At the point when the three-stage matrix voltage is uneven, the key positive-succession voltage vector shows up as a dc voltage on the dq+1 tomahawks of the positive-arrangement SRF and as air conditioning voltages at double the principal utility recurrence on the dq−1 tomahawks of the negative-grouping SRF. Interestingly, the negative

arrangement voltage vector will bring about a dc segment on the negative-grouping SRF and an air conditioner wavering on the positive succession SRF. Since the adequacy of the swaying on the positive-succession SRF matches the dc level on the negative grouping SRF and the other way around, a decoupling system is connected to signals on the dq positive/negative SRF tomahawks with a specific end goal to counterbalance such air conditioning motions. Low-pass channels (LPFs) in Fig.2.3. are in charge of separating the dc segment from the flag on the decoupled SRF tomahawks. These dc parts gather data about the sufficiency and stage point of the positive-and negative-succession segments of the matrix voltage vector.

At long last, the PI controller of the DDSRF PLL chips away at the decoupled q-hub flag of the positive-succession SRF (v*q+1) and plays out an indistinguishable capacity from in a SRF PLL, adjusting the positive-arrangement voltage with the d-pivot. This flag is free of air conditioning parts because of the impact of the decoupling systems; the transfer speed of the circle controller can be thus expanded.

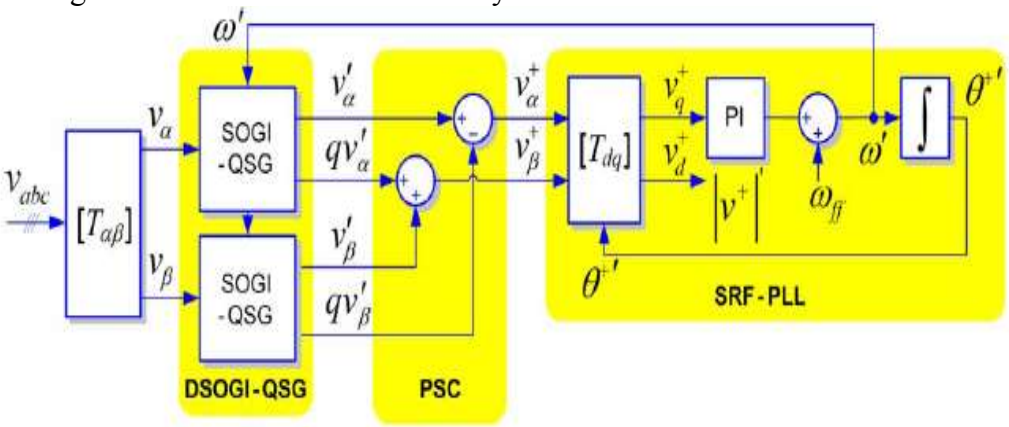

Figure.2.4. DSOGI-PLL block diagram.

This near review well represents the prevalence of SOGI based PLL over DSRF PLL. The working standard of the DSOGI PLL for assessing the positive-and negative-grouping parts of the matrix voltage vectors depends on utilizing the immediate symmetrical segment (ISC) strategy on the αβ stationary reference outline, as clarified in. The chart of the DSOGI PLL is appeared in Fig.2.4. As it can be seen, the ISC strategy is actualized by the positive-succession count piece.

To apply the ISC strategy, it is important to have an arrangement of signs, vα –vβ , speaking to the info voltage vector on the αβ stationary reference outline together with another arrangement of signs, qvα –qvβ , which are in quadrature and slacked concerning vα –vβ . In the DSOGI PLL, the signs to be provided to the ISC technique are acquired by utilizing a double second request summed up integrator (DSOGI), which is a versatile band-pass channel in light of the summed up integrator idea.

International Journal of Research
Available at https://edupediapublications.org/journals
p-ISSN: 2348-6848
e-ISSN: 2348-795X
Volume 03 Issue 18
December 2016

A customary SRF PLL is connected on the evaluated positive-arrangement voltage vector, v+αβ, to make this synchronization system recurrence versatile. Specifically, the v+αβ voltage vector is meant the pivoting SRF, and the flag on the q-hub, v+q , is connected at the contribution of the circle controller. As an outcome, the key network recurrence (ω') and the stage point of the positive-grouping voltage vector (θ+') are assessed by this circle. The evaluated recurrence for the basic matrix segment is bolstered back to adjust the middle recurrence ω' of the DSOGI.

BLOCK DIAGRAMS AND SIMULATION RESULTS

The outcomes acquired with the proposed three synchronization techniques under lattice blame conditions demonstrated that they give better outcomes contrasted with the as of now existed strategies and this strategies are likewise ready to give system strength and high consonant dismissal limit alongside high blame ride through capacity.

5.1. BEHAVIOR IN CASE OF VOLTAGE SAGS:

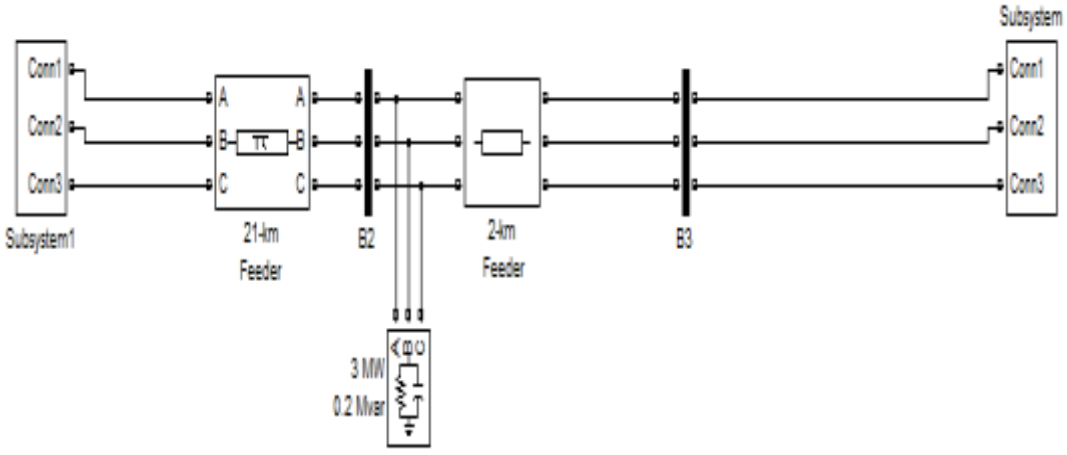

Figure: 5.1.BLOCK DIAGRAM OF VOLTAGE SAGS

Above block diagram represents the block of four types of sags. namely,

- **Type "A" Sag Test:** This kind of voltage sag appears as a consequence of three-phase faults that give rise to high short circuit currents and, hence, to a balanced voltage drop in the network. As Fig. 5(e) and (i) shows, the DDSRF PLL and the DSOGI PLL produce a good response, as both systems achieve a very fast detection (20 ms) of the positive-sequence components (less than two cycles). The response of the 3phEPLL, depicted in Fig. 12(m), also shows a good response, but

with a larger transient in the positive-sequence estimation.

Below mentioned simulation graph is the sag voltage magnitude under type-A sag

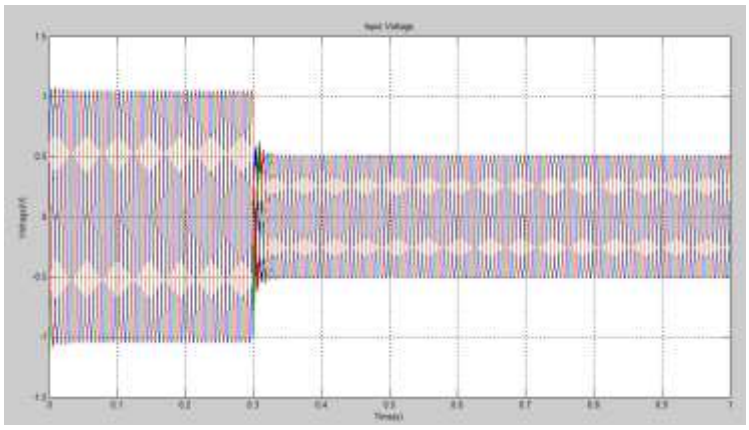

Figure.5.2.simulationof3-phase sag(Type-A)

- **Type "B" Sag Test:** This kind of fault permits analyzing the behavior of the PLLs under test in the presence of zero-sequence components at the input. The Clarke transformation used in DSOGI PLL and DDSRF PLL to extract the $\alpha\beta$ components enhances the response of this synchronization system when the faulty grid voltage presents zero-sequence components. Their responses, as shown in Fig. 5.16 and 5.19, are fast and accurate. On the other hand, the 3phEPLL does not cancel out the zero-sequence component from the input voltage, some-thing which may affect the dynamics of the positive-sequence estimation loop. However, this effect is further attenuated by the computational unit, as Fig. 5.22. shows; the steady-state response is also reached with no great delay, as detailed in Fig. 5.22, showing the good behavior of this PLL under these conditions.

Below simulation graph shows the sag voltage magnitude of the system under type-B sag.

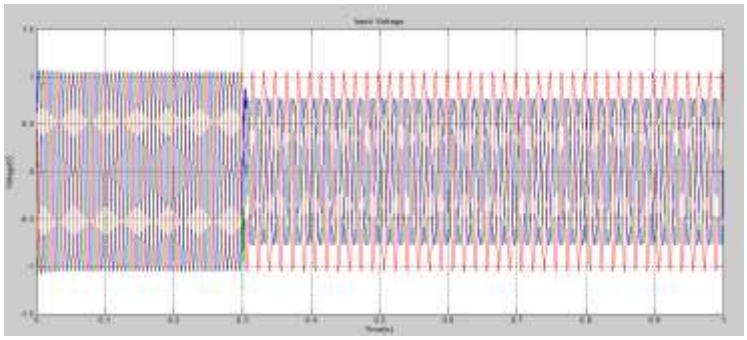

Figure.5.3.simulation of two phase sag-1(Type-B)

□Type "C" and "D" Sag Tests: These sorts of droops show up because of stage to-ground and stage to-stage shortcircuits at the essential twisting of the transformer, individually, as appeared in Table 4.1. In a dispersion system, these bends are more regular than the past ones, as they are the average matrix shortcomings brought about by lightning storms. As delineated in Fig. 5.26&5.36,5.29&5.39, each of the three PLLs allow recognizing the positive arrangement somewhere around 20 and 30 ms; notwithstanding, the 3phEPLL has a slower adjustment, as appeared in Fig. 5.32 and 5.42. This impact is more detectable with the "C" hang, where the blend of the stage bounce and the extent change of two stages happen, as appeared in Fig. 5.32.

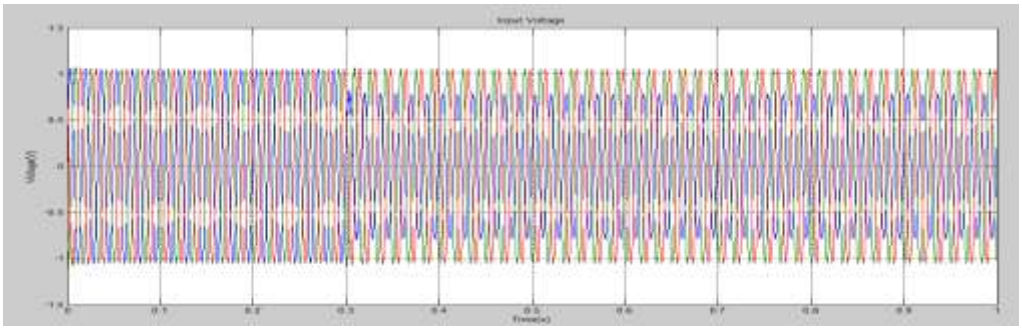

Figure.5.4.simulation of single phase sag(Type-C)

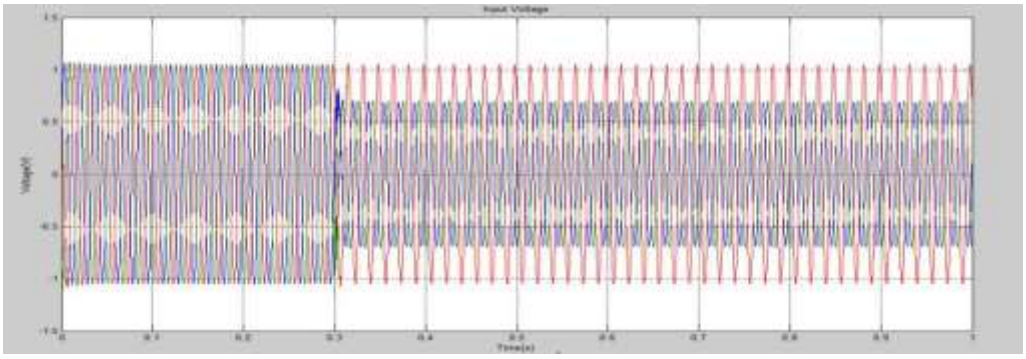

Figure.5.5. Simulation of 2-phase sag-2(Type-D)

5.2. MITIGATION OF SAGS USING DDSRF-PLL:

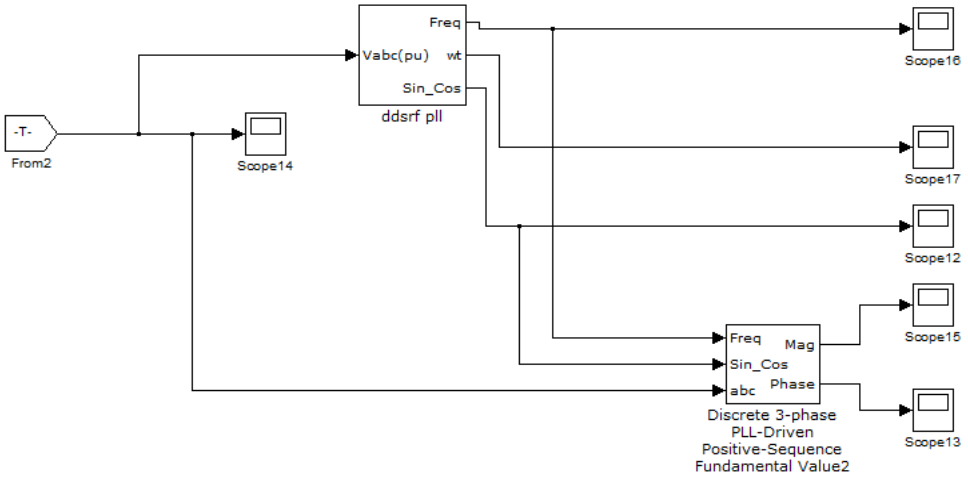

5.6. Block diagram for DDSRF-PLL

The following Simulation results shows the mitigation of four types of sags using DDSRF-PLL synchronization technique

5.2.1. Simulation results of 3-phase sag:

The graph shows voltage magnitude of DDSRF PLL under 3-phase sag, here we can observe a abrupt drop at 0.3 magnitude

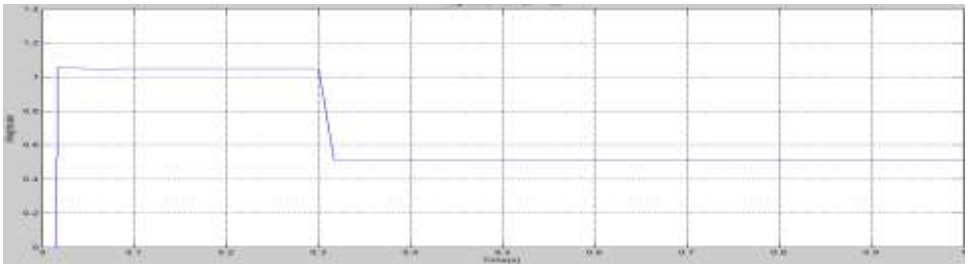

Figure.5.7.voltage magnitude of DDSRF PLL under 3-ph sag

The graph shows phase angle of DDSRF PLL under 3-phase sag, here we can observe a slight drop at 0.3 magnitude.

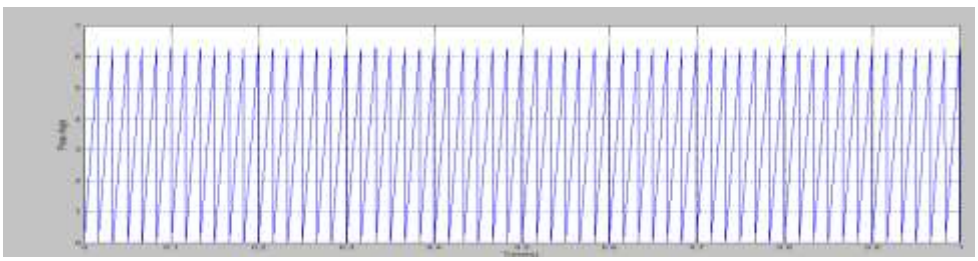

Figure.5.8.phase value of DDSRF PLL under 3-ph sag

The graph shows frequency value of DDSRF PLL under 3-phase sag,here we can observe variations in the frequency.

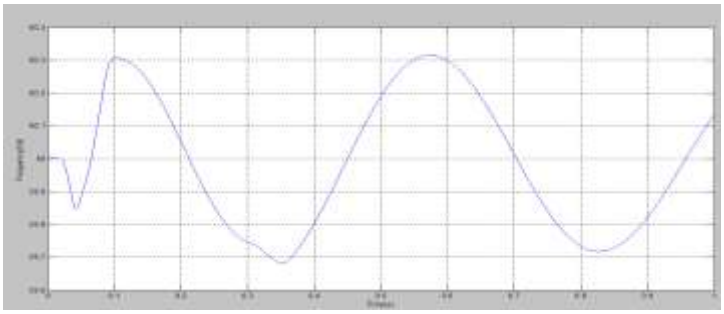

Figure:5.9. Frequency value of DDSRF-PLL under 3-ph sag

5.2.2. simulation results of 2-phase sag-1:

The below graph shows voltage magnitude of DDSRF PLL under 2-phase sag-1,here we can observe more fluctuated drop in voltage level.

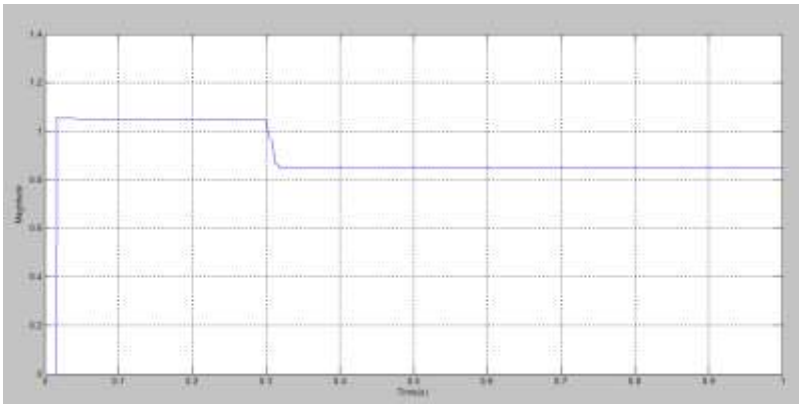

Figure.5.10. Voltage magnitude of DDSRF PLL under 2-phase sag-1(Type-B)

The below graph shows phase magnitude of DDSRF PLL under 2-phase sag-1, here we can observe a fluctuating phase at 0.3 magnitude.

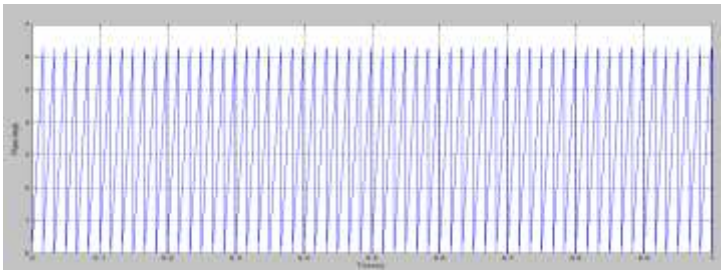

Figure.5.11. phase value of DDSRF PLL under 2p-phase sag-1

The below graph shows frequency value of DDSRF PLL under 2phase sag -1, here we can observe fluctuating frequency magnitude.

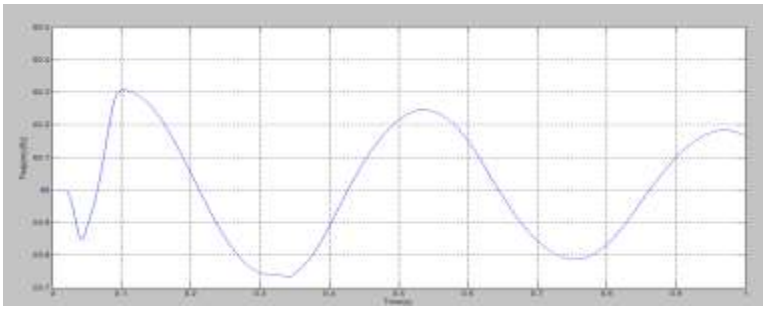

Figure.5.12. Frequency value of DDSRF PLL under 2-phase sag-1

5.2.3. Simulation results of 1-phase sag:

The underneath diagram indicates voltage greatness of DDSRF PLL under 1-stage hang, here we can watch diminished voltage extent.

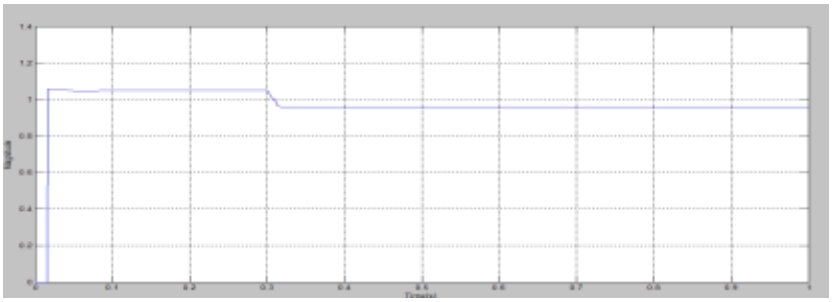

Figure.5.13. Voltage magnitude of DDSRF PLL under 1-ph sag(Type-c)

The underneath chart demonstrates that the reproduction aftereffects of DDSRF PLL under 1-stage list, here we can watch an adjustment in stage esteem at 0.3 greatness

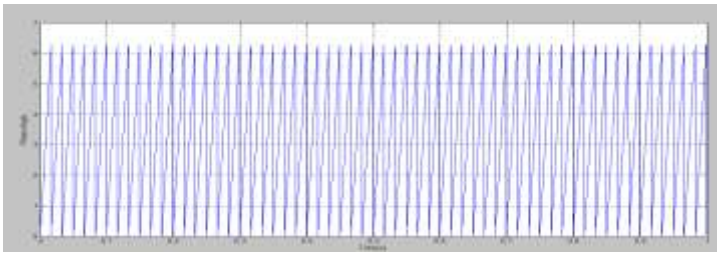

Figure.5.14. phase value of DDSRF PLL under 1-ph sag

The underneath diagram demonstrates reproduction consequence of DDSRF PLL under 1-stage hang, here we can watch that a fluctuating recurrence level at 0.3 greatness.

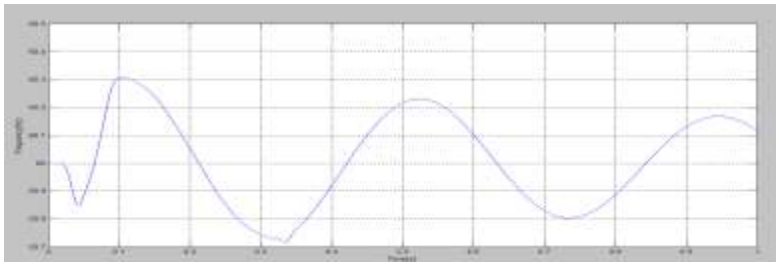

Figure.5.15. Frequency value of DDSRF PLL under 1-ph sag

5.2.4. Simulation results of 2-phase sag -2:

The beneath chart indicates recreation aftereffect of DDSRF PLL under 2-stage droop 2, here we can watch that a fluctuating drop in voltage extent at 0.3-0.35 and afterward stagnant

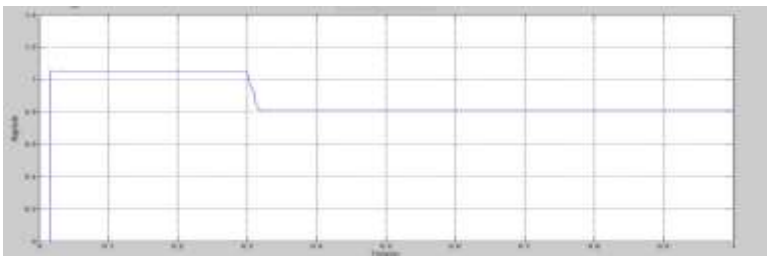

Figure.5.16. Voltage magnitude of DDSRF PLL under 2-phase sag-2(Type-D)

The below graph shows the simulation results of DDSRF PLL under 2-phase sag-2, here we can observe that a phase value

variation. 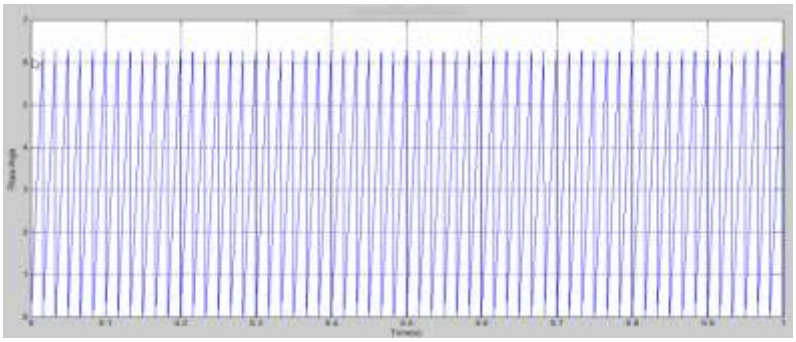

Figure.5.17. phase value of DDSRF PLL under 2- phase sag-2

The underneath graph shows the simulation result of DDSRF PLL under 2-phase sag-2, here we can observe a variation in frequency value after 0.3 magnitude.

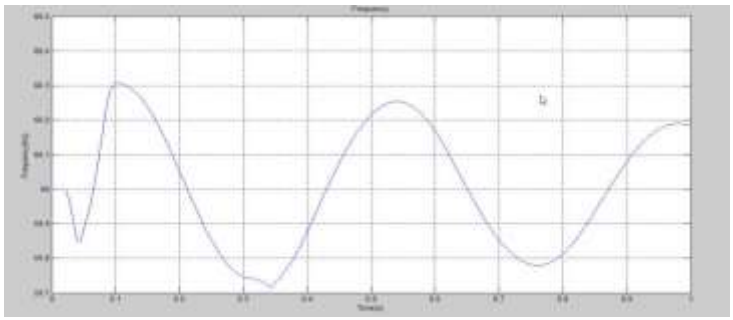

Figure.5.18. Frequency value of DDSRF PLL under 2-phase sag-2

The DDSRF-PLL synchronization technique gives successful yield under adjusted

3-stage systems furthermore diminishes sounds. Be that as it may, amid lopsided systems it is wasteful.

5.3. MITIGATION OF SAGS USING DSOIG PLL

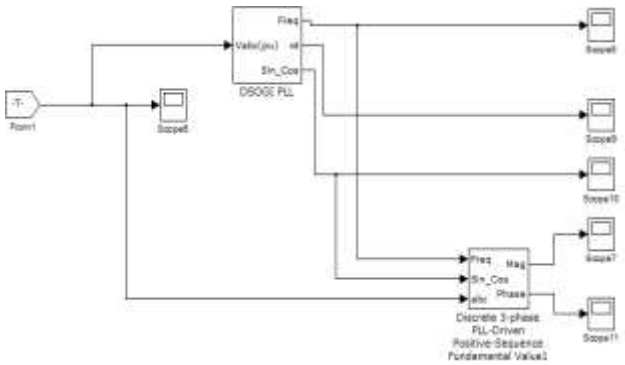

5.19. Block diagram for DSOGI PLL

The following simulation results shows different types of sags mitigation using DSOGI-PLL.

5.3.1. Simulation results of DSOIG PLL:

The graph shows voltage magnitude of DSOIG PLL under 3-phase sag, here we can observe a abrupt steep drop at 0.3 magnitude.

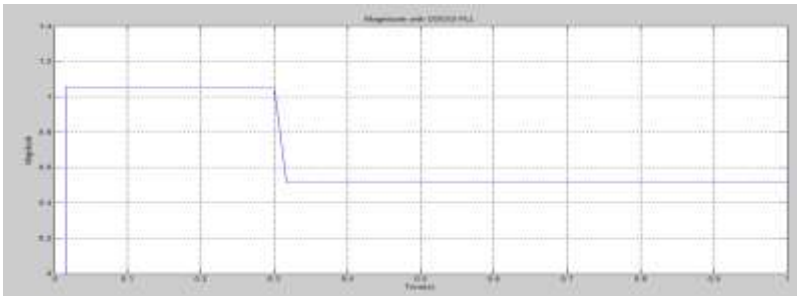

Figure.5.20. voltage magnitude of DSOIG PLL under 3-ph sag

The graph shows phase angle of DSOIG PLL under 3-phase sag, here we can observe a slight drop at 0.3 magnitude.

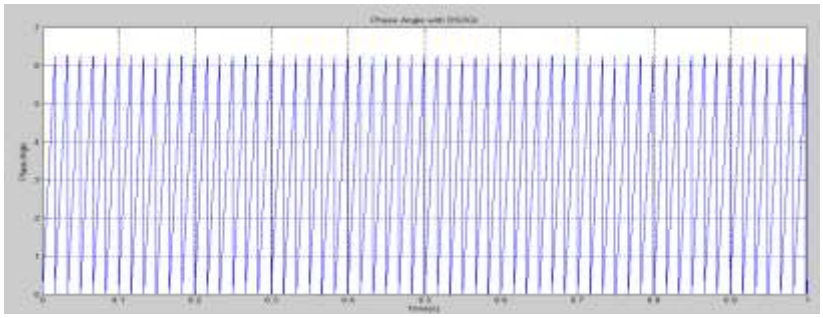

Figure.5.21. Phase value of DSOIG PLL under 3-ph sag

The diagram demonstrates recurrence estimation of DSOIG PLL under 3-stage list, here we can watch substantial varieties in the recurrence.

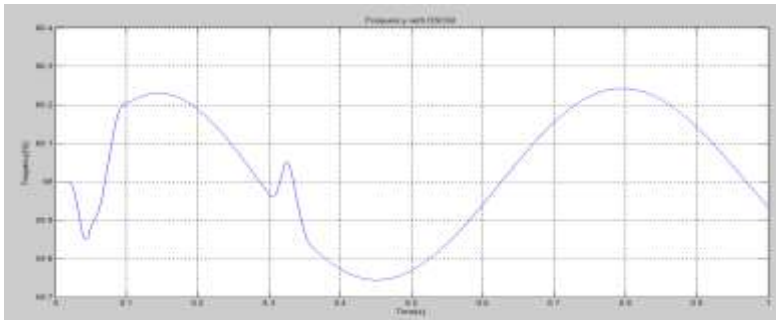

Figure.5.22. Frequency value of DSOIG PLL under 3-ph sag

5.3.2. Simulation results of 2-phase sag-1:

The below graph shows voltage magnitude of DSOIG PLL under 2-phase sag-1, here we can observe more fluctuated drop in voltage level.

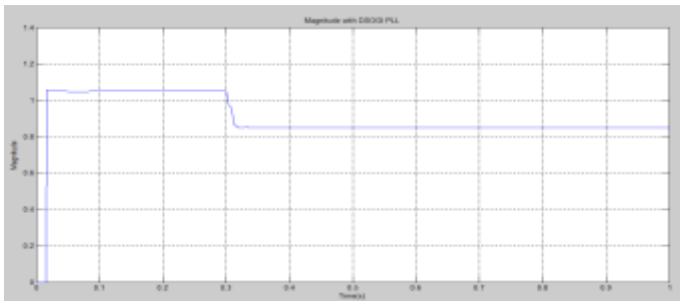

Figure.5.23. Voltage magnitude of DSOIG PLL under 2-phase sag-1

The below graph shows phase magnitude of DSOIG PLL under 2-phase sag-1, here we can observe a fluctuating phase at 0.3 magnitude.

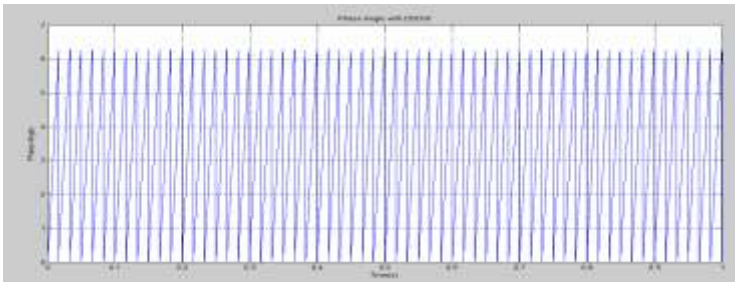

Figure.5.24. phase value of DSOIG PLL under 2-phase sag-1

The below graph shows frequency value of DSOIG PLL under 2phase sag -1, here we can observe fluctuating frequency magnitude.

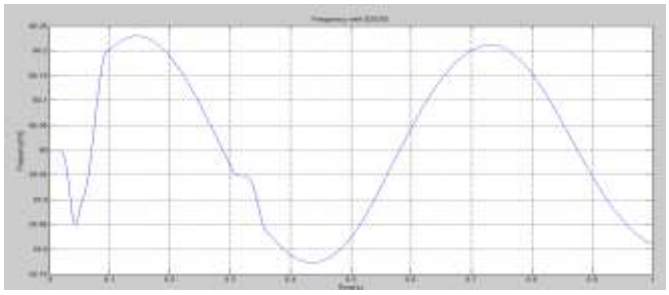

Figure.5.25.Frequency value of DSOIG PLL under 2-phase sag-1

5.3.3. Simulation results of 1-phase sag:

The below graph shows voltage magnitude of DSOIG PLL under 1-phase sag, here we can observe decreased voltage magnitude.

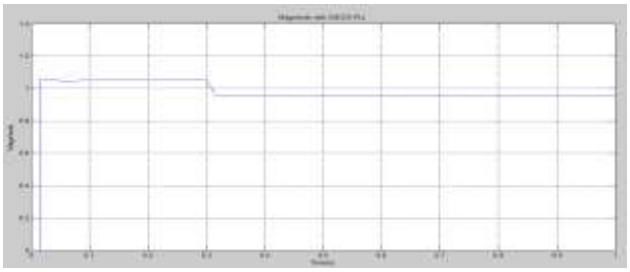

Figure.5.26. voltage magnitude of DSOIG PLL under 1-ph sag

The below graph shows that the simulation results of DSOIG PLL under 1-phase sag, here we can observe a change in phase value at 0.3 magnitude.

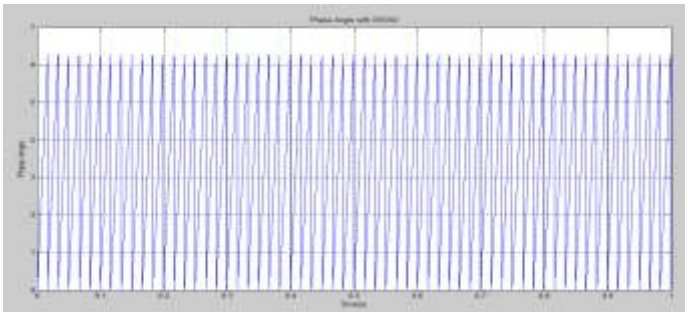

Figure.5.27. phase value of DSOIG PLL under 1-ph sag

The below graph shows simulation result of DSOIG PLL under 1-phase sag, here we can observe that a fluctuating frequency level at 0.3 magnitude.

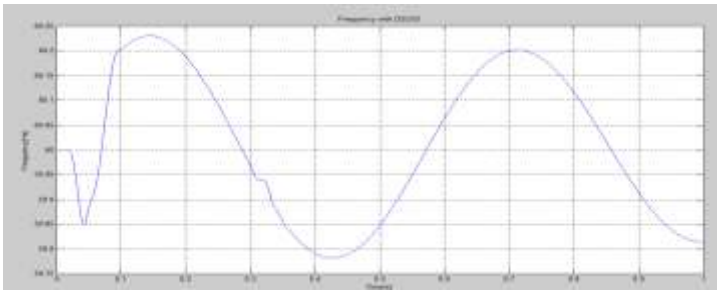

Figure.5.28. Frequency value of DSOIG PLL under 1-ph sag

5.3.4. Simulation results of 2-phase sag-2:

The below graph shows simulation result of DDSRF PLL under 2-phase sag-2, here we can observe that a fluctuating drop in voltage magnitude at 0.3-0.35 and then stagnant.

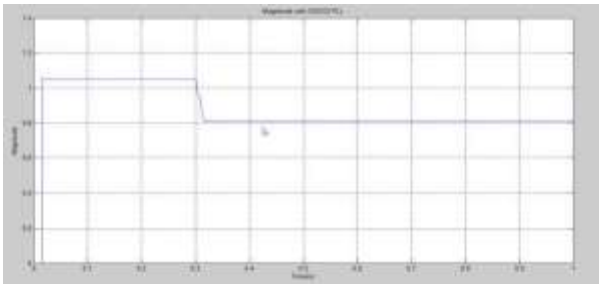

Figure.5.29. Voltage magnitude of DSOIG PLL under 2-phase sag-2

The below graph shows the simulation results of DDSRF PLL under 2-phase sag-2, here we can observe that a phase value variation.

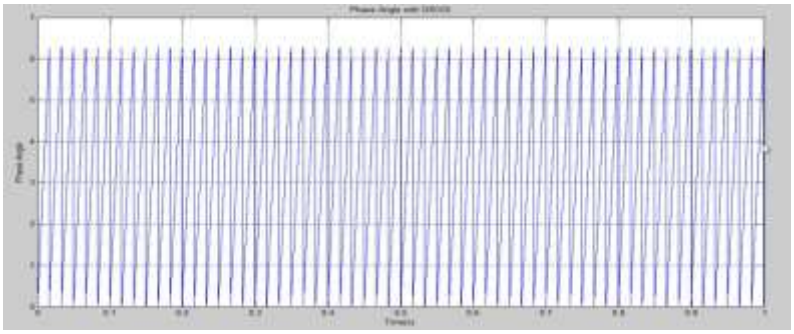

Figure.5.30. Phase value of DSOIG PLL under 2-phase sag-2

The below graph shows the simulation result of DSOIG PLL under 2-phase sag-2, here we can observe a variation in frequency value after 0.3 magnitude.

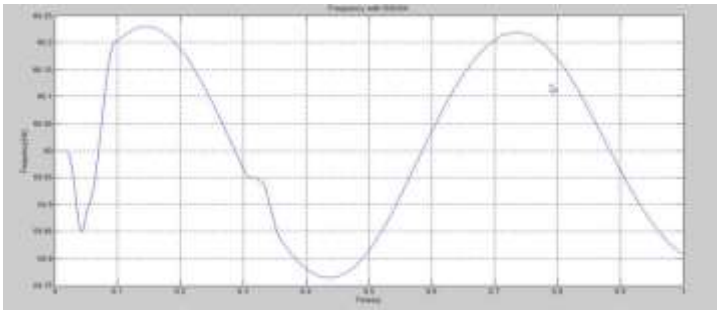

Figure.5.31. Frequency value of DSOIG PLL under 2-phase sag-2.

This method gives both positive and negative sequence voltages for systems and it also gives high harmonic rejection capacity compare to previous method. It gives accurate results under both balanced and unbalanced situations.

MITIGATION OF SAGS USING 3phase-EPLL:

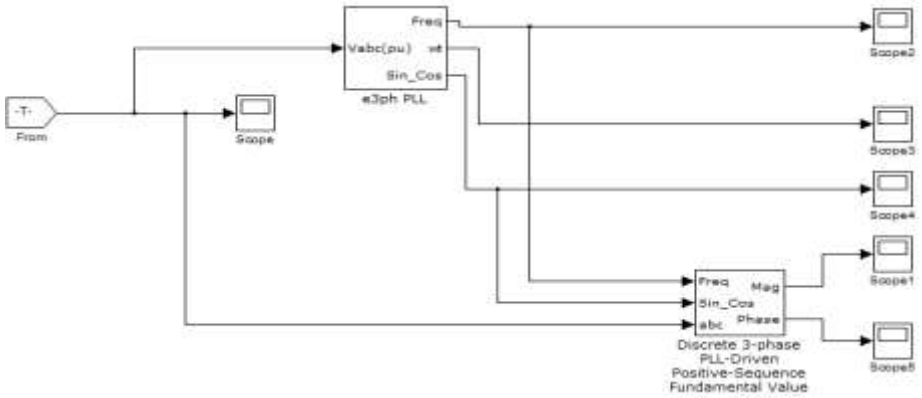

5.32. Block diagram for 3phEPLL

5.4.1. Simulation results of 3-phase sag:

The graph shows voltage magnitude of 3-phase EPLL under 3-phase sag, here we can observe a steep drop at 0.3 magnitude.

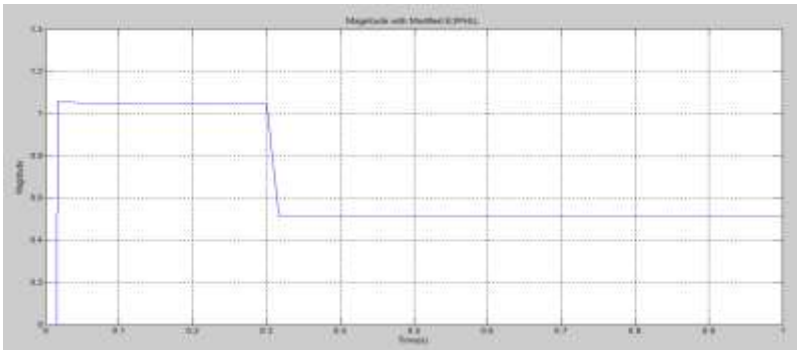

Figure.5.33. voltage magnitude of 3-ph EPLL under 3-ph sag

The graph shows phase angle of 3-phase EPLL under 3-phase sag, here we can observe a slight drop at 0.3 magnitude.

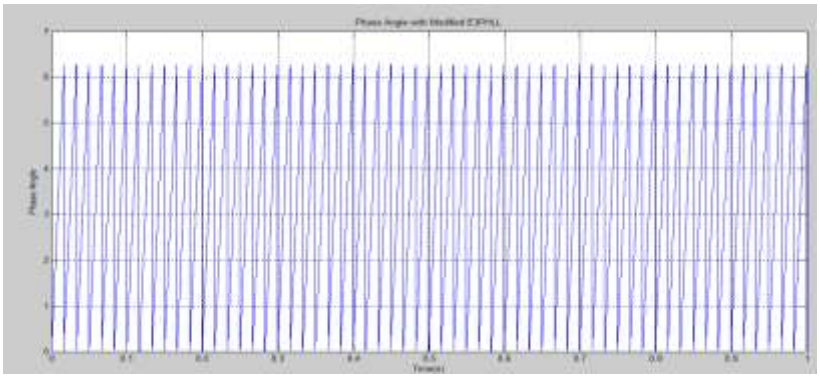

Figure.5.34.Phase value of 3-ph EPLL under 3-ph sag

The graph shows frequency value of 3-phase EPLL under 3-phase sag, here we can observe variations in the frequency.

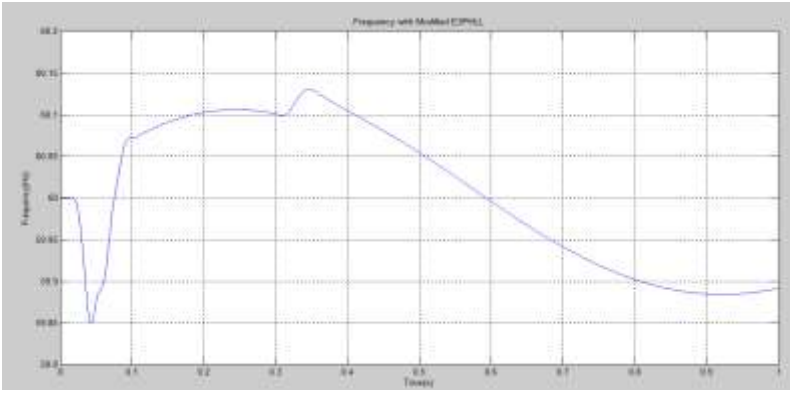

Figure.5.35.Frequency value of 3-ph EPLL under 3-ph sag

5.4.2. Simulation results of 2-phase sag-1:

The below graph shows voltage magnitude of 3-phase EPLL under 2-phase sag-1, here we can observe more fluctuated drop in voltage level.

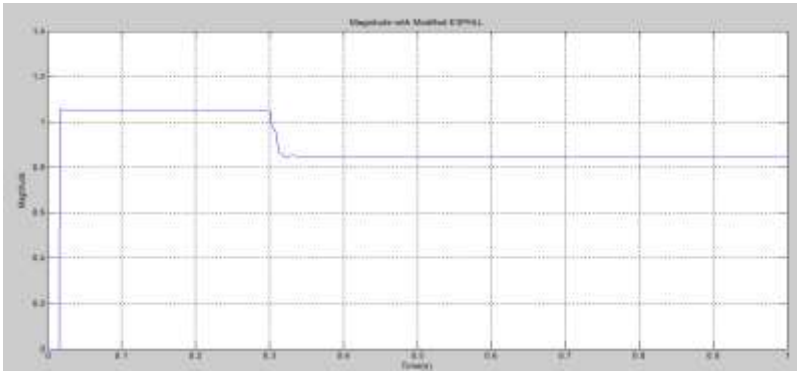

Figure.5.36. Voltage magnitude of 3-ph EPLL under 2-phase sag-1

The below graph shows phase magnitude of 3-phase EPLL under 2-phase sag-1, here we can observe a fluctuating phase at 0.3 magnitude.

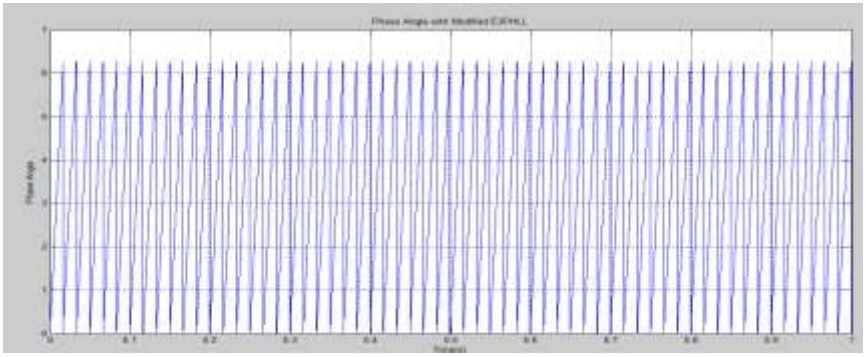

Figure.5.37. Phase value of 3-ph EPLL under 2-phase sag-1

The below graph shows frequency value of 3-phase EPLL under 2phase sag -1, here we can observe fluctuating frequency magnitude at 0.3.

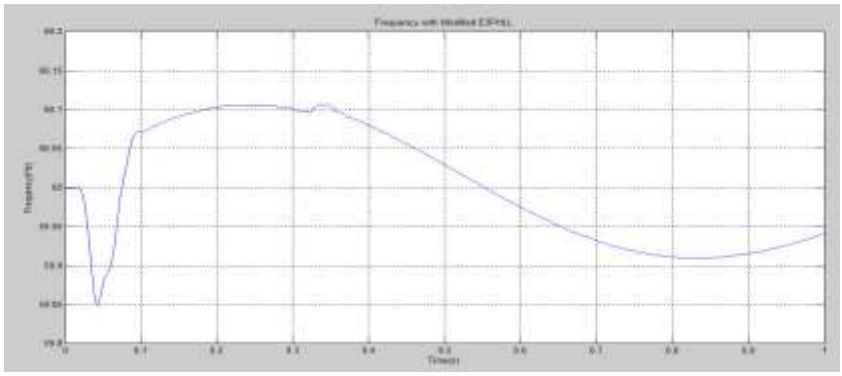

Figure.5.38. Frequency value of 3-ph EPLL under 2-phase sag-1

5.4.3. Simulation results of 1-phase sag:

The below graph shows voltage magnitude of 3-phase EPLL under 1-phase sag, here we can observe decreased voltage magnitude.

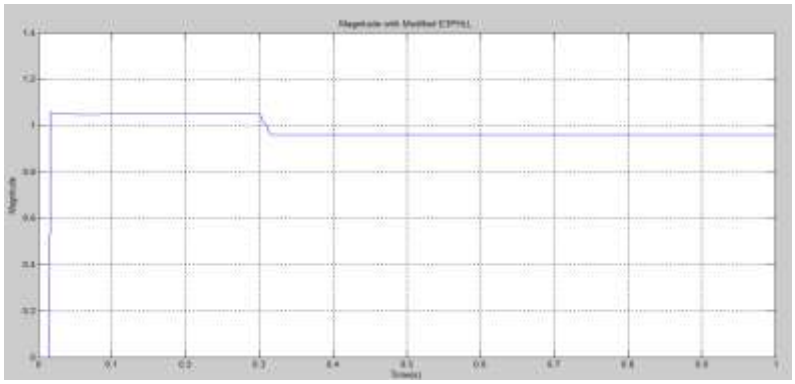

Figure.5.39. Voltage magnitude of 3-ph EPLL under 1-ph sag

The below graph shows that the simulation results of 3-phase EPLL under 1-phase sag, here we can observe a change in phase value at 0.3 magnitude.

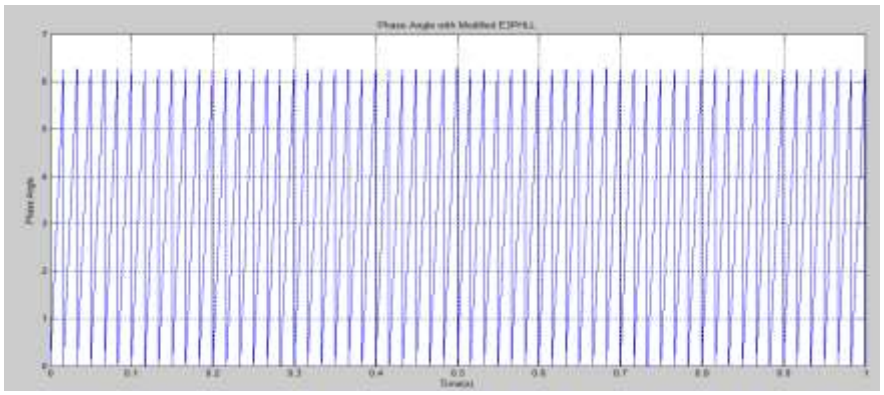

Figure.5.40. phase value of 3-ph EPLL under 1-ph sag

The below graph shows simulation result of 3-phase EPLL under 1-phase sag, here we can observe that a fluctuating frequency level at 0.3 magnitude

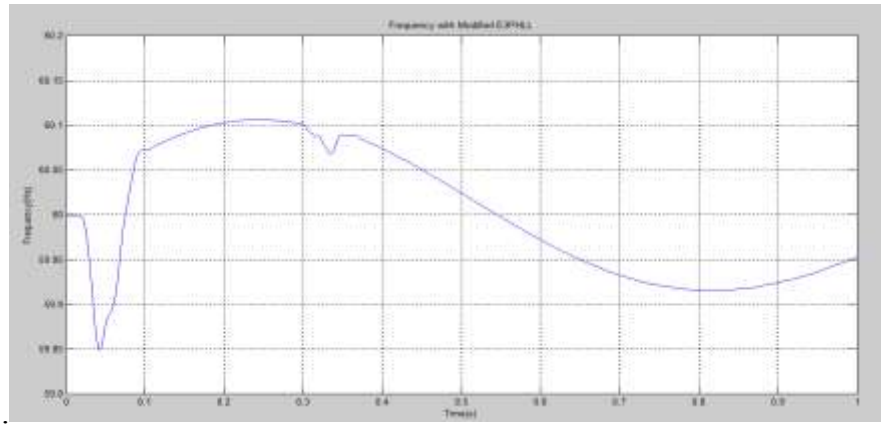

Figure.5.41. Frequency value of 3-ph EPLL under 1-ph sag

Simulation results of 2-phase sag-2:

The below graph shows simulation result of 3-phase EPLL under 2-phase sag-2, here we can observe that a fluctuating drop in voltage magnitude at 0.3-0.35 and then stagnant.

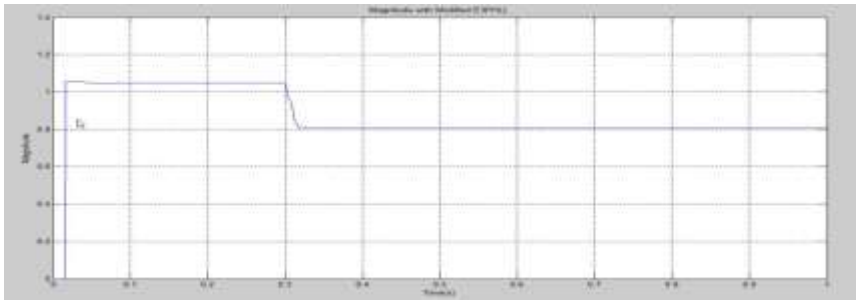

Figure.5.42. Voltage magnitude of 3-ph EPLL under 2-phase sag-2

The below graph shows the simulation results of 3-phase EPLL under 2-phase sag-2, here we can observe that a phase value variation.

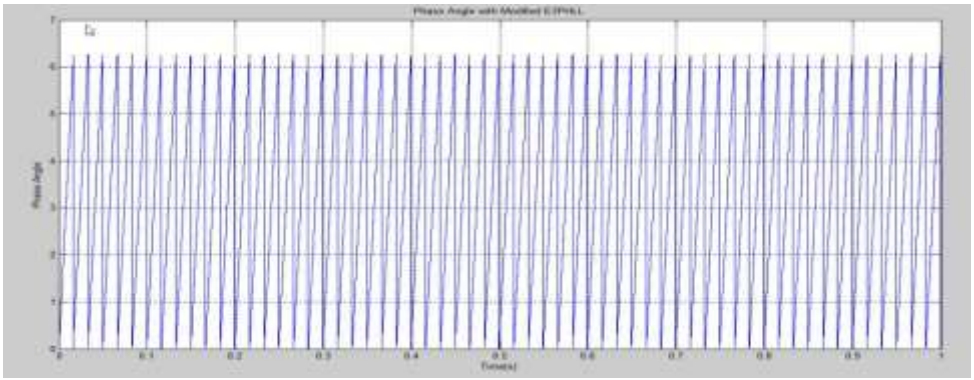

Figure.5.43. phase value of 3-ph EPLL under 2-phase sag-2

The below graph shows the simulation result of 3-phase EPLL under 2-phase sag-2, here we can observe a variation in frequency value after 0.3 magnitude.

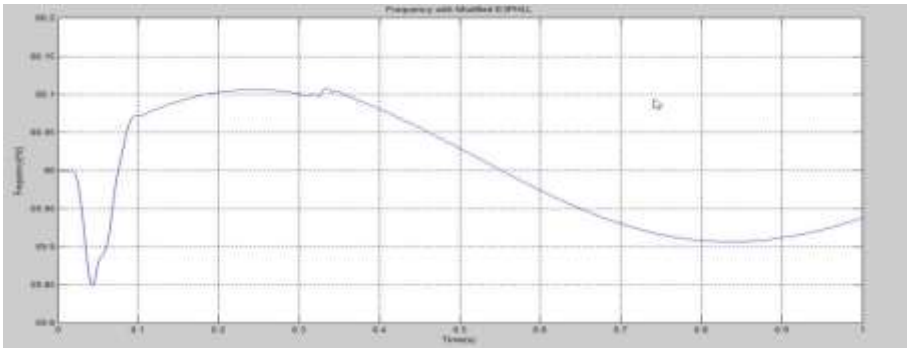

Figure.5.44. Frequency value of 3-ph EPLL under 2-phase sag-2

TABLE5.1: NUMBER OF OPERATIONS PERFORMED BY EACH PLL

Structure	A	M	T	S	D
DDSRF-PLL	22	32	12	14	0
DSOGI-PLL	38	86	4	8	2
3ph EPLL	42	41	19	16	0

A=Addition M=Multiplication T=Trigonometric S=Variable storage D=Division.

Type and number of operations in each PLL. The shadowed cells indicate the synchronization system that is used the least number of times by each operator.

EVALUATION OF THE COMPUTATIONAL BURDEN TIME:

The computational cost in the skimming point TMS320F28335 DSP, which is considered as a microcontroller by the brand itself, has been assessed for every case. Be that as it may, an underlying subjective investigation should be possible if every calculation is isolated into its principal operations. The diverse sorts of fundamental operations, and also how often they were utilized as a part of every calculation, are compressed in Table 5.1., where the shadowed cells show which PLL is utilized the minimum frequently by every administrator.

The outcomes from Table 5.1 appear to demonstrate that the DDSRF PLL and the DSOGI PLL could be the speediest calculations. Then again, the quantity of trigonometrically capacities that the 3phEPLL needs to perform plays against its computational cost. This

announcement can be in this manner affirmed with the trial trouble time measured for each PLL when preparing one cycle, as appeared in Table 5.2.Regarding the aftereffects of Table 5.2, the DDSRF PLL plays out the quickest circle. Regardless of the high number of expansion.

TABLE 5.2: COMPUTATIONAL COST EVALUATION

Structure	Execution time
DDSRF-PLL	5.41μs
DSOIG-PLL	5.91μs
3ph EPLL	8.36μs

Global burden time of one cycle of instructions for each PLL programmed in a TMS320F28335 DSP and multiplications to be calculated, the DSOGI PLL holds second position in this burden-time comparative, although the differences with respect to the DDSRF are not quite significant. Finally, it can be observed that the greatest burden time is obtained with the 3phEPLL.

CONCLUSION:

This paper concentrated the conduct of three propelled network synchronization systems. Their structures have been introduced, and their discrete calculations have been point by point. The DDSRF PLL and the DSOGI PLL permit evaluating the ISCs of a three-stage system working in the αβ reference outline, while the 3phEPLL uses the "abc" reference outline, subsequently working with three factors. As has been appeared, this element disentangles the structure of the DSOGI PLL and the DDSRF PLL, which permits decreasing the computational weight, when contrasted with the 3phEPLL, without influencing its performance.The synchronization capacity of the three PLLs under test has been appeared to be quick and exact under broken situations, permitting the location of the positive succession of the voltage in 20–25 ms in all cases; in any case, the less complex structure of the DDSRF and the DSOGI manages a less demanding tuning of their control parameters and, subsequently, a more precise control of their transient response.The resistance of the dissected PLLs in the likelihood of a dirtied system is better when utilizing the 3phEPLL and the DDSRF, because of their more noteworthy band - pass and low-pass sifting abilities. Despite the fact that the DSOGI likewise offers ascend to sensibly great outcomes, because of its inalienable band-pass separating structure, its reaction is more influenced by sounds.

FUTURE SCOPE:

Though already practiced methods have its advantages, but they are limited by some factors like time consuming, voltage instability, harmonics. The three synchronization methods based on PLL's can be used in distributed generation systems under grid fault conditions using Discretization method in order to enhance the system stability and time reduction capacity. In future the synchronization methods based on

PLL's advance frequency enhanced methods gives us more effective accurate output.

6.3. REFERENCES

[1] A. Zervos and C. Kjaer, Pure Power: Wind Energy Scenarios for 2030. Brussels, Belgium: European Wind Energy Association (EWEA), Apr. 2008. [Online]. Available: http://www.ewea.org/index.php?id=11

[2] F. Blaabjerg, R. Teodorescu, M. Liserre, and A. V. Timbus, "Overview of Control and Grid Synchronization for Distributed Power Generation Systems," IEEE Trans. on Industrial Electronics, vol. 53, no. 5, pp. 1398-1409, 2006.

[3] M. J. Hossain, H. R. Pota, V. Ugrinovskii, and R. A. Ramos, "A novel STATCOM control to augment LVRT capability of fixed-speed induction generators," in 48th IEEE Conference on Decision and Control, Shanghai, China, 16–18 December 2009, pp. 7843–7848.

[4] Francisco D. Freijedo, Jesus Doval-Gandoy, Oscar Lopez, Carlos Martinez-Penalver, Alejandro G. Yepes, Pablo Fernandez-Comesana, Andres Nogueiras, JanoMalvar, Nogueiras, Jorge Marcos and Alfonso Lago, "Grid-Synchronization Methods for Power Converters," Proc. of IEEE 35th Annual Conference on Industrial Electronics, IECON 2009, pp. 522 – 529.

[5] FANG Xiong, WANG Yue, LI Ming, WANG Ke and LEI Wanjun, "A Novel PLL for Grid Synchronization of Power Electronic Converters in Unbalanced and Variable-Frequency Environment," Proc. of IEEE International Symposium on Power Electronics for Distributed Generation Systems: pp. 466-471, 2010.

[6] Bo Sun1, Ning-Yi Dai, U-Fat Chio, Man-Chung Wong, Chi-Kong Wong1, Sai-Weng Sin, Seng-Pan U, R. P. Martins," FPGA-based Decoupled Double Synchronous Reference Frame PLL for Active Power Filters" 978-1-4244-8756-1/11/$26.00 c 2011 IEEE

[7] V.Jaya Prakash, K.Kiran Kumar," A Novel Approach To SOGI Grid Synchronization System For Three-Phase Grid-Connected Power Converters Under Unstable Conditions", International Journal of Advanced Trends in Computer Science and Engineering, Vol.2 , No.6, Pages : 108-113 -2013

[8] Rubens M. Santos Filho, Paulo F. Seixas, Porfírio C. Cortizo, Leonardo A. B. Torres, and André F. Souza," Comparison of Three Single-Phase PLL Algorithms for UPS Applications"; IEEE transaction on industrial electronics,vol_55,no:8,Aug:2008

[9] A. Zervos and C. Kjaer, Pure *Power: Wind Energy Scenarios for 2030*. Brussels, Belgium: European Wind Energy Association (EWEA),Apr. 2008. [Online].

[10] e-on, "Grid code—High and extra high voltage," Bayreuth, Germany.Apr. 2006. [Online]. Available:http://www.pvupscale.org/IMG/pdf/D4_2_DE_annex_A-3_EON_HV_grid connection_requirements_ENENARHS2006de.pdf

[11] *PO-12.3 Requisitos de Respuesta Frente a Huecos de Tension de las Instalaciones Eolicas*, Comisión Nacional de Energía, Madrid, Spain, Oct. 2006.

[12] *IEEE Standard for Interconnecting Distributed Resources with Electric Power Systems*, IEEE Std. 1547-2003, 2003.

[13] *The Grid Code: Revision 31*, National Grid Electricity Transmission, Warwick,U.K.,Oct.2008,no.3.[Online].Available:http://www2.nationalgrid.com/uk/industry-information/electricity code/thegridcode/

[14] Elkraft System og Eltra, "Vindmuller tilsluttet net med sprindinger under 100 kv,"Denmark,TF3.2.6,2004.[Online].Available:http://www.energinet.dk/SiteCollectionDocuments/Engelske%20dokumenter/El/Grid%20Code%203.2.5%20Wind%20Turbines%20connected%20above%20100%20kV.pdf

[15] M. Tsili and S. Papathanassiou, "A review of grid code technical requirements for wind farms," *IET Renew. Power Gen.*, vol. 3, no. 3, pp. 308–332, Sep. 2009.

[16] F. Iov, A. Hansen, P. Sorensen, and N. Cutululis, "Mapping of Grid Faults and Grid Codes," Risø Nat. Lab., Roskilde, Denmark, Tech. Rep. Risoe-R-1617, 2007.

[17] A. Luna, P. Rodriguez, R. Teodorescu, and F. Blaabjerg, "Low voltage ride through strategies for SCIG wind turbines in distributed power generation systems," in *Proc. IEEE PESC*, Jun. 15–19, 2008, no. 1, pp. 2333–2339.

[18] D. Xiang, L. Ran, P. J. Tavner, and S. Yang, "Control of a doubly fed induction generator in a wind turbine during grid fault ride-through,"*IEEE Trans. Energy Convers.*, vol. 21, no. 3, pp. 652–662, Sep. 2006.

[19] J. Morren and S. W. H. de Haan, "Ridethrough of wind turbines with doubly-fed induction generator during a voltage dip," *IEEE Trans. Energy Convers.*, vol. 20, no. 2, pp. 435–441, Jun. 2005.

[20] M. Molinas, J. A. Suul, and T. Undeland, "Low voltage ride through of wind farms with cage generators: STATCOM versus SVC," *IEEE Trans.Power Electron.*, vol. 23, no. 3, pp. 1104–1117, May 2008.